IEEE Access
Multidisciplinary ⋮ Rapid Review ⋮ Open Access Journal

Received January 22, 2021, accepted February 2, 2021, date of publication February 8, 2021, date of current version February 16, 2021.

Digital Object Identifier 10.1109/ACCESS.2021.3057618

Distributed Cooperative Relaying Based on Space-Time Block Code: System Description and Measurement Campaign

HIDEKAZU MURATA, (Member, IEEE), AKIHIRO KUWABARA, AND YUJI OISHI
Graduate School of Informatics, Kyoto University, Kyoto 606-8501, Japan

Corresponding author: Hidekazu Murata (murata@i.kyoto-u.ac.jp)

This work was supported by Grants-in-Aid for Scientific Research by Japan Society for the Promotion of Science (JSPS KAKENHI) Grant Number JP20360170.

ABSTRACT In cooperative relaying, intermediate stations are required to enhance the end-to-end transmission performance. The performance of the cooperative relaying scheme has been investigated theoretically and via computer simulations. However, cooperative relaying using transmit diversity techniques in actual environments has not been investigated thus far. This paper presents an experimental system for distributed cooperative relaying using space-time block code and evaluations of its transmission performances in real propagation channels. To this end, four wireless stations—specifically, one source, two relays, and one destination—were developed using analog transceivers and field-programmable gate arrays for real-time digital signal processing. Sample timing and frequency synchronizations among the four wireless stations were established by using the received signals as a reference. The end-to-end error performance of distributed cooperative relaying was compared to those of noncooperative relaying schemes, and the performances of three relaying schemes were evaluated quasisimultaneously in terms of their cumulative distribution functions of the bit-error ratios (BERs). The experimental results indicated that the BER performance of the two-hop distributed cooperative relaying scheme was substantially superior to those of noncooperative two-hop relaying schemes, including a route diversity scheme.

INDEX TERMS Cooperative relaying, measurement campaign, relay network, space-time code, distributed relaying.

I. INTRODUCTION

Cooperative communication is a novel form of wireless communication that requires intermediate stations in addition to the source and destination stations. The advantages of cooperative communication are path-loss and shadowing reductions as well as diversity gain over fading channels. Hence, cooperative communication schemes can improve the end-to-end transmission performance at the expense of additional intermediate (relay) stations. Although most consumer wireless devices currently communicate directly with only a single base station or access point, cooperative communication has become a popular research topic in 5G networks and other applications, such as device-to-device assisted communications [1] and terrestrial-satellite networks [2]. Recently, an unmanned-aerial-vehicle (UAV)-assisted cooperative communication network was investigated [3] to enhance the performance of UAV-aided relay networks by using multiple UAVs.

Depending on the use of relay stations, several relaying schemes are available. A simple relaying scheme that involves a string of relay stations causes significant degradation in the end-to-end error performance over a fading channel. Cooperative relaying can therefore be a solution to this problem. Darsena *et al.* [4] summarized the design and performance of cooperative multiple-input multiple-output relaying. Dohler *et al.* [5] proposed distributed cooperative relaying schemes, where multiple relay stations cooperatively relayed signals from the source station using a space-time block code (STBC) to improve the end-to-end transmission performance. In the STBC-based cooperative relaying scheme, multiple relay stations operate together using the STBC technique so that a receiving station (next relay station or destination station) benefits from the transmit diversity gain. The performance of the STBC-based cooperative relaying scheme was investigated in depth via computer simulations [6]. The results showed that the end-to-end

The associate editor coordinating the review of this manuscript and approving it for publication was Faissal El Bouanani.

error performance is considerably improved by using the STBC-based cooperative relaying scheme. Diem *et al.* [7] applied the STBC-based cooperative relaying scheme in vehicle-to-vehicle scenarios focusing on the medium access control layer and routing protocols and showed that redundant broadcast messages can be reduced by applying this technique. Akhtar *et al.* [8] studied the impact of realistic impairments on the outage performance of STBC-aided cooperative non-orthogonal multiple access communications.

Studies focusing on implementation and measurement have been conducted to investigate cooperative relaying performances in realistic environments [9]–[15]. Eriksson *et al.* [10] used propagation data in outdoor environments for their performance study. By focusing on relay protocols, transmission experiments have been performed in indoor [11], [12] and vehicular [12] scenarios. Ahmad *et al.* [13] studied a hybrid decode-estimate-forward relaying scheme in an indoor environment. However, only a few studies have investigated the performance of cooperative relaying using the STBC technique [14], [15]. For example, Murphy and Sabharwal [14] evaluated the performance of an STBC-based cooperative relaying scheme by using a fading emulator. Hussain *et al.* [15] implemented two relays in a single transceiver to conduct a transmission experiment in an indoor environment.

The STBC technique can achieve full diversity and offers optimal performance improvement when two signals from different transmit antennas have similar average received power. However, in outdoor distributed cooperative relaying scenarios, the average received power at the destination from one relay station is almost always different from that from a different relay station. Therefore, the advantages of STBC-based cooperative relaying need to be investigated, especially for realistic outdoor distributed scenarios.

To clarify this problem, an STBC-based cooperative relaying system was implemented using a field-programmable gate array (FPGA) [16]. The performance of this system was verified for a fading emulator [16], [17]; moreover, an outdoor measurement study was conducted on a campus of Kyoto University [18]. The analytical performance evaluation was described in [17], and the results theoretically support the advantages of the STBC-based cooperative relaying system. The experimental performance agreed with the analytical performance.

In [18], all the stations were established in a field, and the performance was measured for the pedestrian use case. It was revealed that the benefit of relaying greatly depended on the antenna heights of the relay stations. Therefore, the performance of STBC-based distributed cooperative relaying was investigated for a high relay-antenna scenario with real-time measurements using vehicles in [19]. To the best of our knowledge, outdoor experimental results for distributed cooperative relaying schemes based on the STBC technique have not been reported except for [19]. In this paper, we describe the details of the experimental system, and reevaluate the measured bit-error ratio (BER) performance of the two-hop distributed cooperative relaying scheme based on STBC and compare it to that of noncooperative (simple) two-hop relaying. Measurements for three relaying schemes were conducted quasisimultaneously to ensure fair comparison of these relaying schemes.

The contributions of this work can be summarized as follows:

1) A real-time STBC-based cooperative relaying system is described.
2) Evaluations conducted in an outdoor environment, in which the relay stations were distributed and the source and relay stations were mobile, are discussed.
3) The performance advantage of the STBC-based cooperative relaying scheme was verified by conducting measurements for both cooperative and non-cooperative relaying schemes quasisimultaneously.

This remainder of this paper is organized as follows: Section II describes the system model of the space-time-coded cooperative relaying scheme. Section III introduces the experimental STBC-based cooperative relaying system. The experimental setup and experimental results are discussed in Sections IV and V, respectively. Finally, the conclusions are presented in Section VI.

II. SYSTEM MODEL

A. SPACE-TIME-CODED COOPERATIVE RELAYING

A two-hop STBC-based cooperative relaying scheme comprises a source station (Source), one pair of dedicated relay stations (Relays 1 and 2), and a destination station (Destination). The Source transmits a complex symbol $x_S[k] \in \mathcal{A}$ at time instant k, where the set $\mathcal{A}$ is a complex constellation. The received signals at Relay i are given as

$$z_i[k] = h_{iS}x_S[k] + n_i[k], \ i \in \{1, 2\}, \tag{1}$$

where h_{iS} and $n_i[k]$ represent the complex channel coefficient from Source to Relay i and an additive complex noise sample at Relay i, respectively.

At each relay station, the signal $z_i[k]$ is detected using an estimated complex channel coefficient $\hat{h}_{iS}$, and the detected symbol is denoted as $\hat{x}_i[k] \in \mathcal{A}$. The Relay i transmits the complex symbol $x_{Ri}[k]$ following Alamouti's STBC rule, where the even-numbered ($k = 2j$) and odd-numbered symbols ($k = 2j+1$) are treated differently, as shown below:

$$x_{R1}[2j] = \alpha_1\hat{x}_1[2j] \tag{2}$$

$$x_{R1}[2j+1] = -\alpha_1\hat{x}_1^*[2j+1] \tag{3}$$

$$x_{R2}[2j] = \alpha_2\hat{x}_2[2j+1] \tag{4}$$

$$x_{R2}[2j+1] = \alpha_2\hat{x}_2^*[2j] \tag{5}$$

where α_i is a real number related to the transmit power control, and the superscript $(.)^*$ represents the complex-conjugate operation.

At Destination, the received signal $z_D[k]$ is given by

$$z_D[k] = h_{D1}x_{R1}[k] + h_{D2}x_{R2}[k] + n_D[k], \tag{6}$$

TABLE 1. Transmit amplitude coefficients for the three relaying schemes.

	α_1		α_2	
Verify by CRC	No error	Error	No error	Error
(i) via Relay 1	1	0	0	0
(ii) via Relay 2	0	0	1	0
(iii) Coop	$\frac{1}{\sqrt{2}}$	0	$\frac{1}{\sqrt{2}}$	0

where $h_{\mathrm{D}i}$ and $n_{\mathrm{D}}[k]$ represent a complex channel coefficient from Relay i to Destination and an additive complex noise sample at Destination, respectively. An STBC decoder at Destination multiplies the received signal vector $\left[\, z_{\mathrm{D}}[2j] \;\; z_{\mathrm{D}}^{*}[2j+1] \,\right]^{\mathrm{T}}$ by a matrix as shown below, where the superscript $(.)^{\mathrm{T}}$ represents the transpose operation. The signal vector for detection is given as

$$\begin{bmatrix} z'_{\mathrm{D}}[2j] \\ z'_{\mathrm{D}}[2j+1] \end{bmatrix} = \begin{bmatrix} \hat{h}_{\mathrm{D1}} & \hat{h}_{\mathrm{D2}} \\ \hat{h}_{\mathrm{D2}}^{*} & -\hat{h}_{\mathrm{D1}}^{*} \end{bmatrix}^{\mathrm{H}} \begin{bmatrix} z_{\mathrm{D}}[2j] \\ z_{\mathrm{D}}^{*}[2j+1] \end{bmatrix} \tag{7}$$

where $\hat{h}_{\mathrm{D}i}$ represents the estimated channel coefficient from Relay i to Destination; the operation $(.)^{\mathrm{H}}$ represents the Hermitian transpose of a matrix. For simplicity, perfect channel estimation is assumed, so that (7) becomes

$$\begin{bmatrix} z'_{\mathrm{D}}[2j] \\ z'_{\mathrm{D}}[2j+1] \end{bmatrix} = \begin{bmatrix} \alpha_1\, h_{\mathrm{D1}} & \alpha_2\, h_{\mathrm{D2}} \\ \alpha_2\, h_{\mathrm{D2}}^{*} & -\alpha_1\, h_{\mathrm{D1}}^{*} \end{bmatrix}^{\mathrm{H}} \begin{bmatrix} z_{\mathrm{D}}[2j] \\ z_{\mathrm{D}}^{*}[2j+1] \end{bmatrix}. \tag{8}$$

Therefore, ignoring the noise terms, $z'_{\mathrm{D}}[2j]$ and $z'_{\mathrm{D}}[2j+1]$ are given as

$$\begin{aligned} z'_{\mathrm{D}}[2j] = {} & \alpha_1^2 |h_{\mathrm{D1}}|^2 \hat{x}_1[2j] + \alpha_2^2 |h_{\mathrm{D2}}|^2 \hat{x}_2[2j] \\ & + \alpha_1 \alpha_2 h_{\mathrm{D1}}^{*} h_{\mathrm{D2}} \left(\hat{x}_2[2j+1] - \hat{x}_1[2j+1] \right), \end{aligned} \tag{9}$$

and

$$\begin{aligned} z'_{\mathrm{D}}[2j+1] = {} & \alpha_1^2 |h_{\mathrm{D1}}|^2 \hat{x}_1[2j+1] + \alpha_2^2 |h_{\mathrm{D2}}|^2 \hat{x}_2[2j+1] \\ & + \alpha_1 \alpha_2 h_{\mathrm{D1}} h_{\mathrm{D2}}^{*} \left(\hat{x}_1[2j] - \hat{x}_2[2j] \right), \end{aligned} \tag{10}$$

respectively. These signals are used for detection at Destination. As can be seen from (9) and (10), intersymbol interference (ISI) is observed if the detected symbols at the two relay stations are not identical.

B. RELAYING SCHEMES

In this study, three half-duplex decode-and-forward relaying schemes are considered, and it is assumed that there is no feedback channel to Source. At Relay i, the detected symbols $\hat{x}_i[k] \in \mathcal{A}$ in a packet are verified using a cyclic redundancy check (CRC) code. The three relaying schemes used in this work are

(i) simple relaying via Relay 1 (via Relay 1),
(ii) simple relaying via Relay 2 (via Relay 2), and
(iii) cooperative relaying via Relays 1 and 2 (Coop).

The transmit amplitude coefficients α_1 and α_2 for the three relaying schemes are shown in Table 1. In all three schemes, the packets with errors will not be forwarded ($\alpha_i = 0$); therefore, there is no ISI at Destination. Cooperative diversity gain is achieved in the cooperative relaying scheme only when no errors are found in both relay stations. Note that the total transmit powers of Relays 1 and 2 are identical for the aforementioned three relaying schemes.

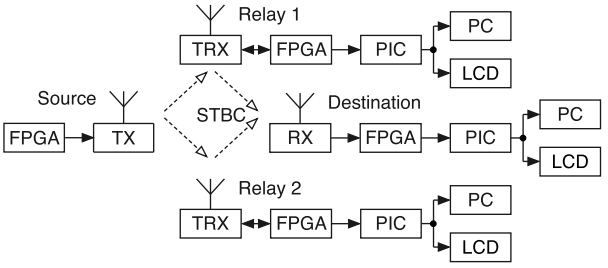

FIGURE 1. Experimental system.

TABLE 2. Major parameters of the measurement system.

Parameter	Value
Carrier frequency	1.299 GHz
Intermediate frequency	10.85 MHz
Modulation scheme	$\pi/4$ shift QPSK
Symbol rate	21.1914 kHz
Antenna (Source & Destination)	Omni-directional (5.5 dBi) 1.76 m height
Antenna (Relays 1 & 2)	Omni-directional (14.9 dBi)
Antenna height (Relay 1)	29 m
Antenna height (Relay 2)	35 m
RF output power (Source)	30 dBm
RF output power (Relays 1 & 2, (i) and (ii))	30 dBm
RF output power (Relays 1 & 2, (iii))	27 dBm
Transmit and receive filter	Root roll-off Nyquist (Roll-off factor $\alpha = 0.7$)
STBC	Alamouti scheme
Error detection	CRC-16
FPGA	Stratix EP1S25F780C5

III. SYSTEM DESCRIPTION

A. HARDWARE STRUCTURE

Fig. 1 shows the block diagram of the experimental system [16] employed in this work. The Source comprises an FPGA board and analog transmitter (TX). Relays 1 and 2 have analog transceivers (TRX), an FPGA board, a peripheral interface controller (PIC), a liquid crystal display (LCD), and a personal computer (PC) for data recording. The Destination has an analog receiver (RX) instead of the TRX of the relay stations. The major parameters used in the experiments are summarized in Table 2. The frequency closest to the main cellular bands was chosen as far as radio licenses were available to us. The transmit power was set to be within the license range and the symbol rate was set so that the signal would experience frequency flat fading.

The PIC calculates the BER and received signal strength indicator (RSSI) based on information from the FPGA and the TRX or RX. These values are displayed on the LCD and sent to the PC via a universal serial bus. The PC records these data but does not process the signals or control the equipment.

B. TRANSMITTER

The block diagram of the transmitter is shown in Fig.2. The FPGA board includes a nine-stage pseudonoise (PN) generator, CRC encoder, quadrature phase-shift keying (QPSK) mapper, finite impulse response (FIR) filter, numerically controlled oscillator (NCO) circuit, multiplier, and 14-bit digital-to-analog (D/A) converter. When the transceiver operates in

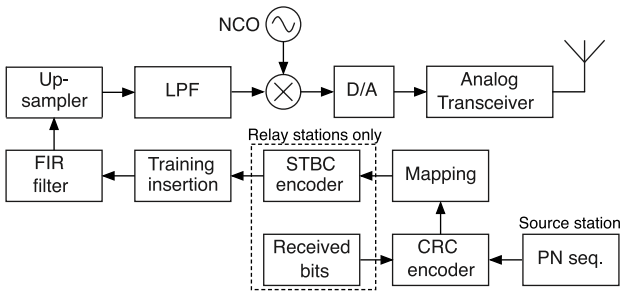

FIGURE 2. Block diagram of the transmitter.

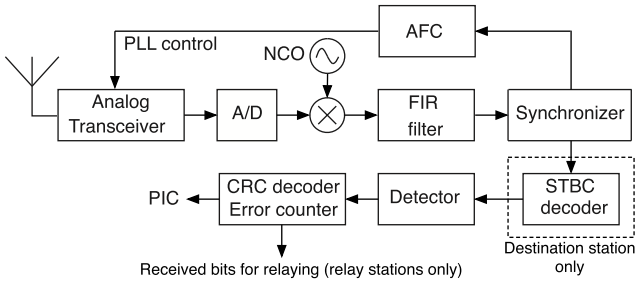

FIGURE 3. Block diagram of the receiver.

the transmit mode, the intermediate frequency (IF) signal is generated by the digital circuits implemented using the FPGA. The TX or TRX upconverts this IF signal to a radio frequency (RF) signal. At the relay stations, the error-free received bits are used for STBC encoding, where unique STBC codes are assigned to the relay stations.

C. RECEIVER

Fig. 3 shows the block diagram of the receiver, where an analog transceiver operating in the receive mode downconverts the received RF signal to the IF signal. In the FPGA, a 12-bit analog-to-digital (A/D) converter samples and quantizes this signal. Using a multiplier, an NCO circuit, and an FIR filter, the digital IF signal is demodulated and fed into a frequency and timing synchronizer. After estimating the channel coefficient using a simple correlation technique, the decision is made at a detector in the relay station. At Destination, the STBC signals are decoded before arriving at the decision. When a packet is determined to be error-free by CRC, the decoded bits are set as the initial value of the PN generator inside the error counter, and the number of bit errors is counted.

D. FRAME STRUCTURE AND PACKET FORMAT

Time-division single carrier frequency relaying is used in the experimental system. The analog transceiver of each relay station operates in two modes: transmit and receive. The transceivers switch between these two modes periodically for relaying the signal. The analog transceiver requires a switching time that is attributable to the electromechanical relay used for transmit/receive switching. Therefore, in the frame format shown in Figs.4(a) and (b), 32 packets are packed into one block so that the transmit/receive switching frequency can be reduced.

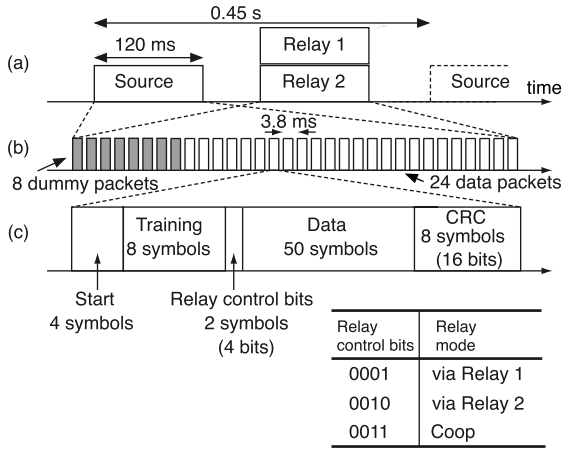

FIGURE 4. Frame structure and packet format.

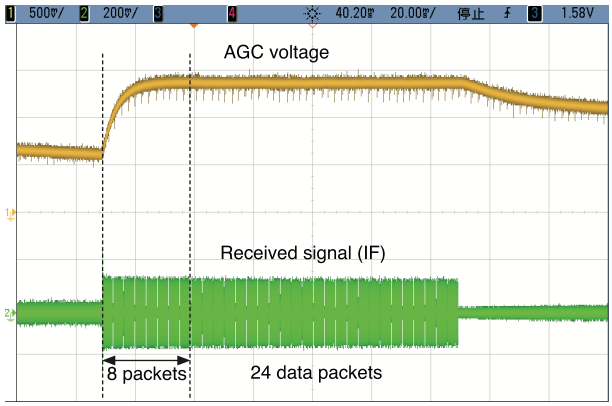

FIGURE 5. AGC voltage and block of packets in the IF signal.

Because the signals are received intermittently in this packet transmission system, the gain of the automatic gain control (AGC) component in the analog transceiver is maximum during the no-signal interval. To prevent signal distortion, eight dummy packets are included at the beginning of the packet block, and these packets are excluded from BER calculation at the target. The next 24 packets are data packets that are used for BER calculation. The time constant of the AGC is about 20 ms, as shown in Fig. 5. Therefore, eight packets are sufficient for stabilizing the AGC.

As shown in Fig. 4(c), each packet consists of four symbols as the start signal, eight symbols as the training sequence, four bits as the relay control flag, 100 bits as data, and 16 bits as the CRC bits. All wireless stations are assigned a unique orthogonal training sequence. The wireless station identifies the station from which the received signal is sent using the training sequence, which enables it to receive only the desired signals.

In this study, the performances of the three relaying schemes are evaluated. Field measurements conducted for the three relaying schemes show that the results depend on channel conditions, which are inevitably different for

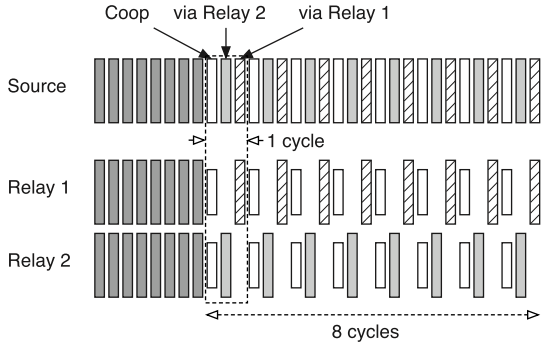

FIGURE 6. Relaying packets with transmit power control.

each scheme. To ensure fair comparison, we examine the three relaying schemes for three consecutive packets, as shown in Fig. 6. Thus, it may be said that the performances of the three relaying schemes are measured quasisimultaneously. The relaying schemes are controlled according to the relay control bits in the packet.

E. TIMING AND FREQUENCY SYNCHRONIZATIONS

Timing and frequency synchronizations are crucial for the STBC technique. In the field measurements, the Source and Destination move around in an urban area. Therefore, both the frequency and timing reference signals cannot be shared by wiring. Thus, the proposed solution involves two relay stations and a destination station that synchronize the symbol timings and frequencies autonomously with the received signal.

Based on signal correlation between the training sequence and received signal from the source, the relay stations determine the symbol timings for demodulation according to the conventional procedure. The relay stations control the transmission timings in 6 μs steps according to these symbol timings. Therefore, the destination will receive the time-aligned signals from both relay stations.

An automatic frequency control (AFC) circuit is used to estimate the carrier frequency offset via observed phase rotations of the estimated complex channel coefficients between adjacent packets. If the phase is constantly rotated, the AFC circuit regulates the phase-locked loop (PLL) circuit of the analog transceiver in steps of 1 Hz, thus establishing frequency synchronization.

F. IN-LAB PERFORMANCE VERIFICATION

Fig. 7 shows the BER performance of the experimental system [16]. All the channels were emulated using fading emulators. The amplitudes of the channel coefficient $|h_{iS}|, |h_{Di}|(i = 1, 2)$ follow the independent and identically distributed (i.i.d.) Rayleigh distribution. The maximum Doppler frequency was 1 Hz (Jakes's spectrum). Computer simulation results obtained assuming perfect channel estimation and perfect timing and frequency synchronization are also plotted in this figure. A noise figure of 5.5 dB was also considered in the simulation.

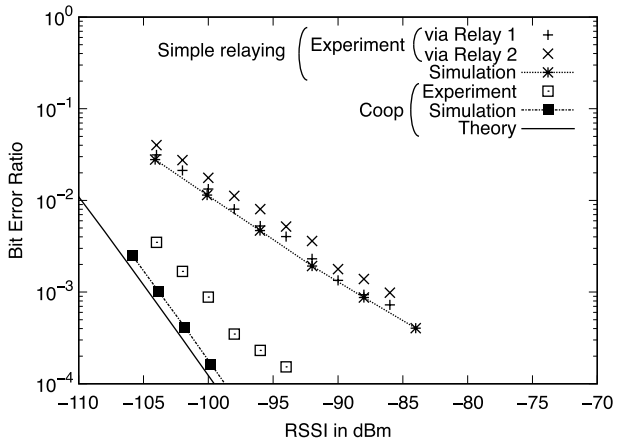

FIGURE 7. BER performance of the experimental system. All four channels are i.i.d. Rayleigh fading channels. Average received signal powers at Relays 1 & 2 and Destination are equal. ©IEICE [16] Fig. 13.

As can be seen, the experimental system performs closely to the computer simulation, particularly in the simple relaying case. In the cooperative relaying case, the advantage of cooperative relaying is confirmed. However, BER performance degradation up to 6 dB is observed. This degradation may be due to residual timing and frequency differences between the transmitted signals from Relay 1 and Relay 2.

Fig. 7 also shows the theoretical end-to-end BER performance of cooperative relaying when block fading is assumed. The end-to-end BER $b_{\text{coop}}(\bar{\gamma})$ can be calculated as

$$\begin{aligned} b_{\text{coop}}(\bar{\gamma}) = {} & 0.5\, p(\bar{\gamma})p(\bar{\gamma}) \\ & + 2\, b_{\text{2nd-hop}}(\bar{\gamma}/2)p(\bar{\gamma})(1 - p(\bar{\gamma})) \\ & + b_{\text{STBC}}(\bar{\gamma})(1 - p(\bar{\gamma}))(1 - p(\bar{\gamma})), \end{aligned} \tag{11}$$

where $b_{\text{2nd-hop}}(\bar{\gamma})$ and $b_{\text{STBC}}(\bar{\gamma})$ are the well-established BERs of QPSK and STBC coded QPSK, respectively. In this BER calculation, the packet error ratio $p(\bar{\gamma})$ is approximated by [20]

$$p(\bar{\gamma}) = 1 - \exp\left(-\frac{k_2}{\bar{\gamma}}\right) n^{\left(-\frac{k_1}{\bar{\gamma}}\right)}, \tag{12}$$

where $k_1 = 1/1.0636$, $k_2 = -1.241$, and $\bar{\gamma}$ and n are the average SNR and packet length, respectively.

IV. EXPERIMENTAL SETUP

A. MEASUREMENT SCENARIO

As shown in Fig. 8, the four stations were spatially separated. Source and Destination were mobile, and their antennas were mounted atop moving vehicles; the antennas of both Source and Destination were situated at a height of 1.76 m above the ground. These stations moved along the routes shown in Fig. 8. Relay 1 was fixed atop a five-story building within the campus of Kyoto University, and its antenna was placed at a height of 29 m above the ground. Relay 2 was fixed atop an eight-story building in the same campus, and its antenna was situated at a height of 35 m above the ground.

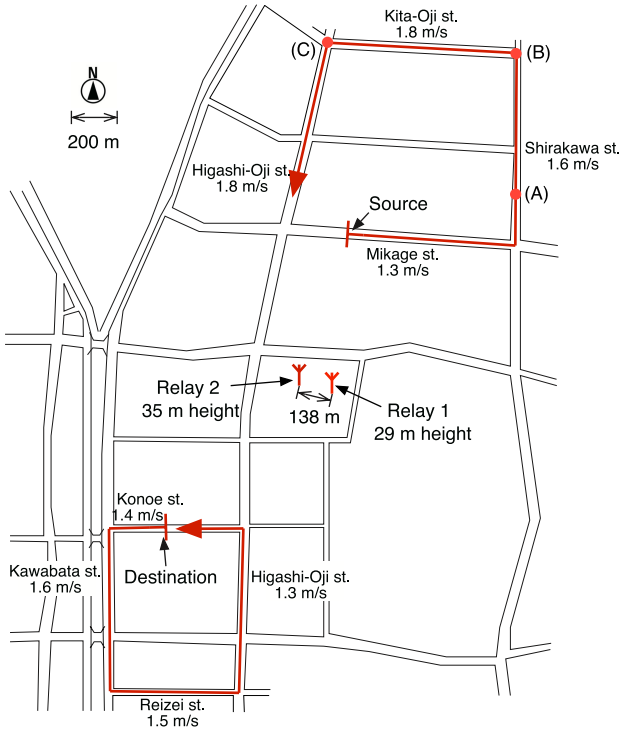

FIGURE 8. Locations of the relay stations and mobile routes of the Source and Destination.

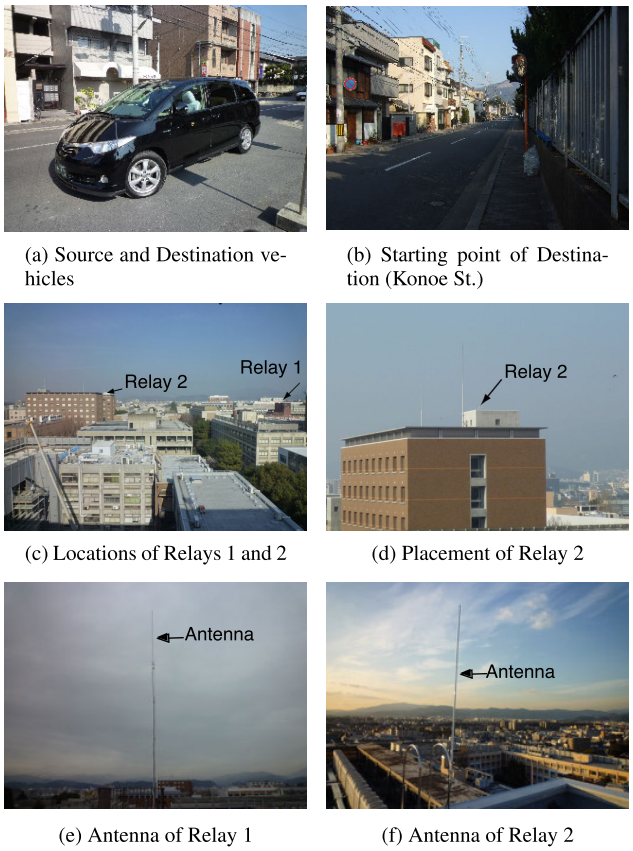

(a) Source and Destination vehicles
(b) Starting point of Destination (Konoe St.)
(c) Locations of Relays 1 and 2
(d) Placement of Relay 2
(e) Antenna of Relay 1
(f) Antenna of Relay 2

FIGURE 9. Experimental layout depicting the placement locations of the antennas within the campus of Kyoto University.

The routes for the mobile antennas were determined through a preliminary experiment to ensure that the average received signal strengths at the relay stations and destination station were greater than −100 dBm. Fig. 9 depicts the locations and placement of the antennas.

The BER performance and RSSI were measured and recorded at the two relay stations as well as the destination station once every second. The RSSI was derived from the maximum AGC voltage of the analog receiver over a one-second duration. Therefore, this RSSI provided an approximate value of the received power and did not distinguish between the transmitting relay stations or the relaying schemes.

B. REMOTE MONITORING SYSTEM

For the measurement campaign, the four wireless stations were placed away from each other, and a remote monitoring system was developed to ensure appropriate operation. This software-based system utilized a mobile operator network to broadcast and gather information about the current positions, BERs, and RSSIs from the four wireless stations shown in Fig. 10. Relays 1 and 2 were fixed atop buildings, and the Source and Destination antennas were mounted atop moving vehicles. A screenshot of the user interface of the software employed for remote monitoring is presented in Fig. 11. Using this system, the operations staff at the four different locations shared the current statuses of their measurement activities, including the positions of the moving vehicles.

V. EXPERIMENTAL RESULTS

The measurement campaign was conducted in the vicinity of Kyoto University, Sakyo Ward, Kyoto City, Japan. The Source and Destination vehicles moved as slowly as possible and occasionally stopped at the traffic lights. While these vehicles were in motion, the measurement setups were used to record the BERs and RSSIs of the three relaying schemes every second. The average speeds of the Source and Destination vehicles are shown in Fig. 8.

Figs. 12 and 13 show the BER and RSSI performances at Relays 1 and 2, respectively. Observing the RSSI fluctuations, all four channels clearly suffered from shadowing and fading. The BERs are approximately between 10^{-3} and 10^{-2} for most of the time at both relay stations. In both figures, the three periods from (A) 10′05″ (10 minute 5 seconds) to 10′35″, (B) 16′11″ to 16′41″, and (C) 24′09″ to 25′00″ are marked as gray sections. In (A) and (B), the BERs at both relay stations are less than 10^{-4}, and the RSSI is relatively stable; this is because the Source vehicle stopped at traffic lights at (A) and (B), as shown in Fig. 8. In (C), however, the BER at Relay 2 is larger, whereas that at Relay 1 is less than 10^{-4}. Thus, the propagation path from Source to Relay 2 experienced considerable fading.

The BER performances and RSSIs at the Destination for the three relaying schemes are shown in Fig. 14. In Fig. 14, it is observed that the BER performance of

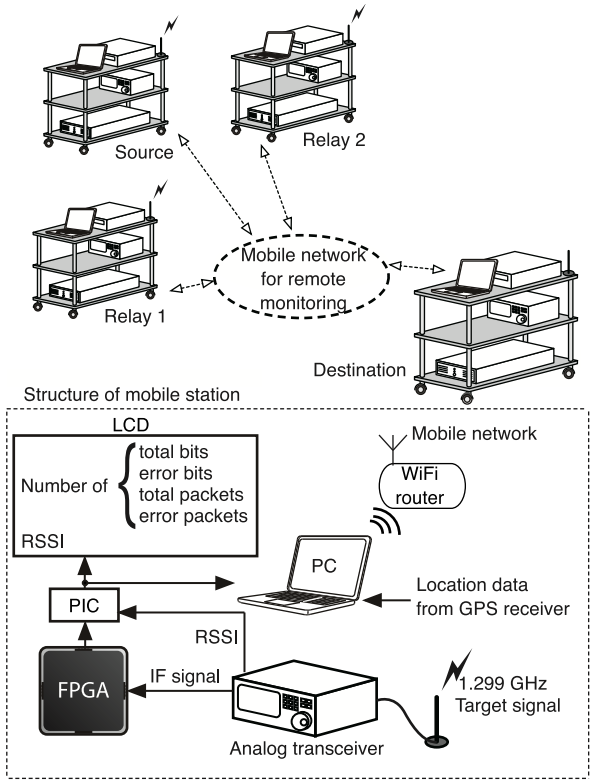

FIGURE 10. Experimental setup and remote monitoring system.

FIGURE 11. Remote monitoring software using mobile network.

(iii) Coop is almost always better than those (i) via Relay 1 and (ii) via Relay 2, which are noncooperative relays. In particular, in (A), the BER at the Destination is less than 10^{-4} irrespective of the relaying scheme used. In (B), bit errors are observed in both (i) via Relay 1 and (ii) via Relay 2. In contrast, (iii) Coop enables better BER owing to the cooperative diversity gain. In (C), the BER at the Destination is better than those for (i) via Relay 1 and (ii) via Relay 2. In this period (C), some errors can be observed at Relay 2, as shown in Fig. 13. However, the packets from Relay 2 to Destination helped improve the BER at the Destination.

As seen in Fig. 15, the performance is evaluated in terms of the empirical cumulative distribution function (ECDF) of the BERs at the Destination. This figure includes one more performance metric, namely (iv) route diversity, where the

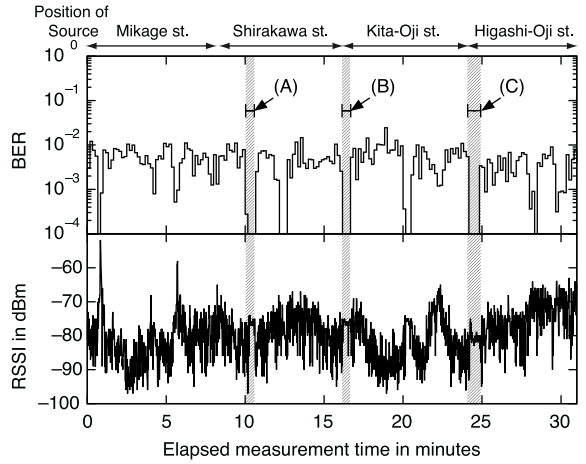

FIGURE 12. BER performance and RSSI at Relay 1.

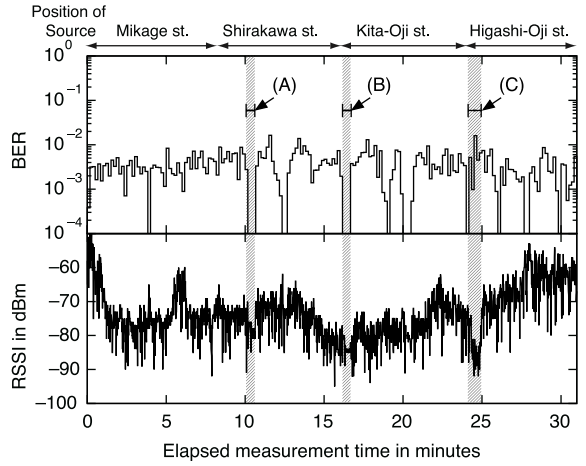

FIGURE 13. BER performance and RSSI at Relay 2.

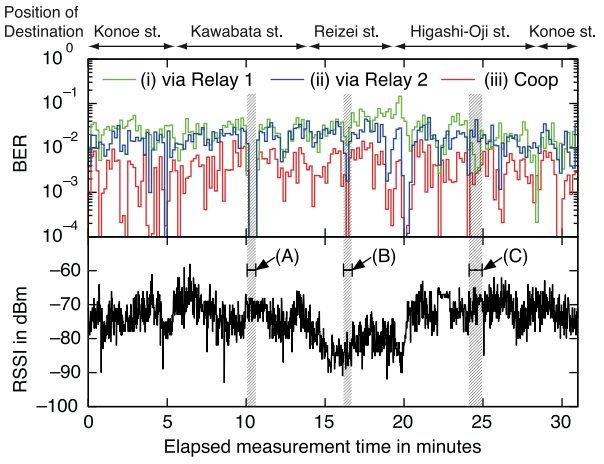

FIGURE 14. BER performance and RSSI at Destination.

recorded BER performances (i) via Relay 1 and (ii) via Relay 2 were used to calculate the final BER by choosing the better relay each second. This relay scheme indicates that the relay

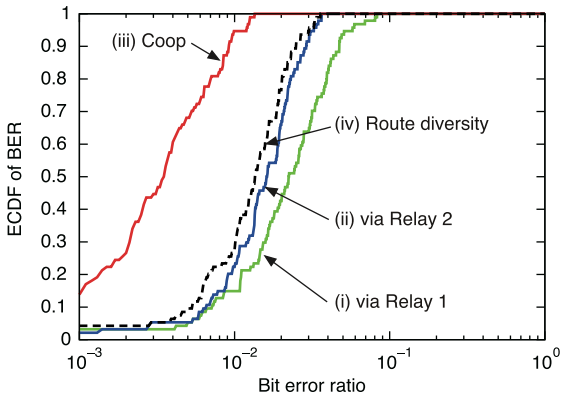

FIGURE 15. ECDF of BER comparisons for the four relaying schemes.

route is switched to the path with the better BER each second. Although the performance of this scheme was evaluated from the measurement results, it was not actually examined in the measurement campaign.

Fig. 15 clearly shows that the performance of (iii) Coop is significantly better than those (i) via Relay 1 and (ii) via Relay 2. Thus, the benefits of distributed cooperative relaying were demonstrated by actual field measurements. For example, the cumulative probability that the BER is less than or equal to 10^{-2} is approximately 0.95 for (iii) Coop and below 0.24 for Relays 1 and 2. Further, the BER performance of (ii) is better than that of (i), which may be attributable to the higher location of the antenna of Relay 2 than Relay 1. The performance of (iv) route diversity is also observed to be better than those of (i) and (ii). However, the route diversity offers limited improvement, and the cumulative probability that the BER is less than or equal to 10^{-2} is approximately 0.30.

VI. CONCLUSION

In this paper, the STBC-based cooperative relaying system was described. Then, the process and results of measurements conducted of two-hop relaying schemes were presented. The measurements were conducted using two vehicles in the vicinity of Kyoto University, Kyoto, Japan. The experimental results showed that the BER performance of the two-hop distributed cooperative relaying scheme based on the STBC was substantially superior to those of noncooperative two-hop relaying schemes, including a route diversity scheme. The results confirmed that STBC-based cooperative relaying can improve end-to-end error performance in realistic environments.

The error performance of the route diversity scheme was derived from the recorded BER performances of the noncooperative relaying schemes. Further study is required for a detailed comparison of the cooperative and route diversity schemes.

REFERENCES

[1] G. I. Tsiropoulos, A. Yadav, M. Zeng, and O. A. Dobre, "Cooperation in 5G HetNets: Advanced spectrum access and D2D assisted communications," *IEEE Wireless Commun.*, vol. 24, no. 5, pp. 110–117, Oct. 2017.

[2] X. Zhu, C. Jiang, L. Kuang, N. Ge, S. Guo, and J. Lu, "Cooperative transmission in integrated terrestrial-satellite networks," *IEEE Netw.*, vol. 33, no. 3, pp. 204–210, May 2019.

[3] S. K. Singh, K. Agrawal, K. Singh, C.-P. Li, and W.-J. Huang, "On UAV selection and position-based throughput maximization in multi-UAV relaying networks," *IEEE Access*, vol. 8, pp. 144039–144050, 2020.

[4] D. Darsena, G. Gelli, and F. Verde, "Design and performance analysis of multiple-relay cooperative MIMO networks," *J. Commun. Netw.*, vol. 21, no. 1, pp. 25–32, Feb. 2019.

[5] M. Dohler, A. Gkelias, and H. Aghvami, "2-hop distributed MIMO communication system," *Electron. Lett.*, vol. 39, no. 18, pp. 1350–1351, Sep. 2003.

[6] T. Yamaoka, Y. Hara, N. Fukui, H. Kubo, and T. Yamazato, "A simple cooperative relaying with Alamouti coded transmission," *IEICE Trans. Commun.*, vols. E95–B, no. 2, pp. 643–646, Feb. 2012.

[7] C.-H. Diem, K. Sato, and T. Fujii, "Cooperative distributed STBC transmission scheme for multi-hop V2V communications," *IEICE Trans. Fundamentals Electron., Commun. Comput. Sci.*, vol. E99.A, no. 1, pp. 252–262, 2016.

[8] M. W. Akhtar, S. A. Hassan, S. Saleem, and H. Jung, "STBC-aided cooperative NOMA with timing offsets, imperfect successive interference cancellation, and imperfect channel state information," *IEEE Trans. Veh. Technol.*, vol. 69, no. 10, pp. 11712–11727, Oct. 2020.

[9] G. J. Bradford and J. N. Laneman, "A survey of implementation efforts and experimental design for cooperative communications," in *Proc. IEEE Int. Conf. Acoust., Speech Signal Process.*, Dallas, TX, USA, Mar. 2010, pp. 5602–5605.

[10] G. Eriksson, S. Linder, and J. Gronkvist, "Measurement-based analysis of two-hop cooperative relaying," in *Proc. IEEE Mil. Commun. Conf. (MILCOM)*, San Diego, CA, USA, Nov. 2013, pp. 538–543.

[11] M. Serror, S. Vaaben, K. Wehrle, and J. Gross, "Practical evaluation of cooperative communication for ultra-reliability and low-latency," in *Proc. IEEE 19th Int. Symp. A, World Wireless, Mobile Multimedia Networks (WoWMoM)*, Chania, Greece, Jun. 2018, pp. 14–15.

[12] S. Valentin, H. S. Lichte, D. Warneke, T. Biermann, R. Funke, and H. Karl, "Mobile cooperative WLANs–MAC and transceiver design, prototyping, and field measurements," in *Proc. IEEE 68th Veh. Technol. Conf.*, Sep. 2008, pp. 1–5.

[13] A. Ahmad, I. Khan, A. N. Hassan, J. Chattha, and M. Uppal, "Design and experimental prototyping of layered hybrid decode-estimate-forward relaying," in *Proc. IEEE 89th Veh. Technol. Conf. (VTC-Spring)*, Kuala Lumpur, Malaysia, Apr. 2019, pp. 1–7.

[14] P. Murphy and A. Sabharwal, "Design, implementation, and characterization of a cooperative communications system," *IEEE Trans. Veh. Technol.*, vol. 60, no. 6, pp. 2534–2544, Jul. 2011.

[15] N. Hussain, K. Ziri-Castro, D. Jayalath, and M. Arafah, "Experimental evaluation of DCOOP protocol using USRP-RIO based testbed at 5.8 GHz," in *Proc. IEEE 84th Veh. Technol. Conf. (VTC-Fall)*, Sep. 2016, pp. 1–6.

[16] H. Murata, Y. Oishi, K. Yamamoto, and S. Yoshida, "FPGA implementation of STBC based cooperative relaying system," *IEICE Trans. Commun.*, vol. E93-B, no. 8, pp. 1988–1992, Aug. 2010.

[17] H. Murata, M. Miyagoshi, and Y. Oishi, "Analytical end-to-end PER performance of multi-hop cooperative relaying and its experimental verification," *IEICE Trans. Commun.*, vol. E100.B, no. 3, pp. 449–455, 2017.

[18] Y. Oishi and H. Murata, "Field experiments of multi-hop cooperative communications using space-time block code," *J. Inst. Image Inf. Telev. Engineers*, vol. 74, no. 2, pp. 412–416, Feb. 2020.

[19] T. Mimura, A. Kuwabara, H. Murata, K. Yamamoto, and S. Yoshida, "Packet transmission experiments of STBC-based multi-hop cooperative relaying," in *Proc. IEEE Int. Conf. Commun. (ICC)*, Kyoto, Japan, Jun. 2011, pp. 1–5.

[20] S. Liu, X. Wu, Y. Xi, and J. Wei, "On the throughput and optimal packet length of an uncoded ARQ system over slow Rayleigh fading channels," *IEEE Commun. Lett.*, vol. 16, no. 8, pp. 1173–1175, Aug. 2012.

HIDEKAZU MURATA (Member, IEEE) received the B.E., M.E., and Ph.D. degrees in electronic engineering from Kyoto University, Kyoto, Japan, in 1991, 1993, and 2000, respectively.

In 1993, he joined the Faculty of Engineering, Kyoto University. From 2002 to 2006, he served as an Associate Professor with the Tokyo Institute of Technology. Since October 2006, he has been with Kyoto University, where he is currently an Associate Professor with the Department of Communications and Computer Engineering, Graduate School of Informatics. His major research interest includes signal processing and its hardware implementation, particularly for application to cooperative wireless networks.

Dr. Murata is a member of the IEICE and ITE. He received the Young Researcher's Award from the IEICE of Japan, in 1997, the Ericsson Young Scientist Award in 2000, the Young Scientists' Prize of the Commendation for Science and Technology from the Minister of Education, Culture, Sports, Science and Technology, in 2006, the Best Paper Award of the IEICE in 2011 and 2013, and the IEEE ICC Best Paper Award in 2014.

AKIHIRO KUWABARA received the B.E. degree in electric and electronic engineering and the M.E. degree in informatics from Kyoto University, Kyoto, Japan, in 2009 and 2011, respectively.

Since 2011, he has been with Fujitsu Ltd., Kanagawa, Japan.

YUJI OISHI received the B.E. degree in electric and electronic engineering and the M.E. degree in informatics from Kyoto University, Kyoto, Japan, in 2008 and 2010, respectively.

Since 2010, he has been with the Research and Development Group, Hitachi Ltd., Kokubunji, Japan.